Published in final edited form as:
Biochemistry. 2010 May 11; 49(18): 3898–3907. doi:10.1021/bi100056v.

The Interfacial Properties of Apolipoprotein B292-593 (B6.4-13) and B611-782 (B13-17). Insights into the Structure of the Lipovitellin Homology Region in ApoB

Libo Wang, **Zhenghui Gordon Jiang**, **C. James McKnight**, and **Donald M. Small***
Department of Physiology and Biophysics, Boston University School of Medicine, Boston, Massachusetts 02118

Abstract

The N-terminal sequence of apolipoprotein B (apoB) is critical in triacylglycerol-rich lipoprotein assembly. The first 17% of apoB (B17) is thought to consist of three domains: B5.9, a β-barrel, B6.4-13, a series of 17 α-helices and B13-17, a putative β-sheet. B5.9 does not bind to lipid while B6.4-13 and B13-17 contain hydrophobic interfaces that can interact with lipids. To understand how B6.4-13 and B13-17 might interact with triacylglycerol during lipoprotein assembly, the interfacial properties of both peptides were studied at the triolein/water interface. Both B6.4-13 and B13-17 are surface active. Once bound the peptides can neither be exchanged or pushed off the interface. Some residues of the peptides can be ejected from the interface upon compression but re-adsorb on expansion. B13-17 binds to the interface more strongly. The maximum pressure the peptide can withstand without being partially ejected (Π_{MAX}) is 19.2mN/m for B13-17 compared to 16.7mN/m for B6.4-13. B13-17 is purely elastic at the interface while B6.4-13 forms a viscous-elastic film. When spread at an air/water interface, the limiting area and the collapse pressures are 16.6Å^2/aa and 31mN/m for B6.4-13, 17.8 Å^2/aa and 35mN/m for B13-17, respectively. The α-helical B6.4-13 contains some hydrophobic helices that stay bound and prevent the peptide from leaving the surface. The β-sheets of B13-17 bind irreversibly to the surface. We suggest that during lipoprotein assembly, the N-terminal apoB starts recruiting lipid as early as B6.4 but additional sequences are essential to form a lipid pocket that can stabilize lipoprotein emulsion particles for secretion.

Apolipoprotein B (apoB) -containing lipoproteins including chylomicrons, very low density lipoproteins (VLDL), intermediate density lipoproteins (IDL) and low density lipoproteins (LDL) are the major carriers of triacylglycerol (TAG) and cholesterol in human plasma (1,2). ApoB is the major non-exchangeable component of these apoB-containing lipoproteins. It exists in two forms in human, the full length of apoB (B100) and the truncated N-terminal 48% of apoB (B48). B100 in liver and B48 in intestine recruit and assemble phospholipids, TAGs and cholesterol to form nascent TAG-rich emulsion particles which are secreted into plasma in the form of VLDL and chylomicrons, respectively. In plasma these lipoproteins are remodeled by the action of lipid exchange proteins and various lipases. Chylomicrons are converted to chylomicron remnants and VLDL is converted to IDL and then LDL. These lipoproteins are taken up mainly in the liver via receptor regulated endocytotic pathways. Elevated levels of apoB-containing lipoprotein particles are a major risk factor for atherosclerosis (1,2). However, adequate apoB is required for transporting TAG and cholesterol in the blood stream to peripheral tissues for energy usage, fat storage, cell membrane synthesis and maintenance, and steroid hormone production. ApoB binds irreversibly to lipid

*To whom correspondence should be addressed: Department of Physiology and Biophysics, Boston University School of Medicine, 700 Albany Street, W-302, Boston, Massachusetts 02118. Tel: 617-638-4001; Fax: 617-638-4041; dmsmall@bu.edu.

and has an extensive conformational flexibility to fulfill the need to cover and stabilize the lipoprotein particles of varied sizes and different lipid and apolipoprotein compositions (3-7).

B100 is a huge glycoprotein consisting of 4536 amino acid residues with a molecular mass of 550 kDa. Electron Micrographs of ApoB solubilized in sodium deoxycholate micelles shows a 650Å-long flexible beaded ribbon of varied width (8). In Electron Microscopy reconstructions LDL particles appear to be quasi spherical particles approximately 220-240 Å in diameter with a high density protein ring surrounding a low density lipid core (9). The N-terminal appears to form a domain projecting from the surface. It is generally accepted that apoB can be divided into five super domains: NH2-βα1-β1-α2-β2-α3-COOH (10-12). The α2, α3 and the β1, β2 domains comprise predominantly amphipathic α helix (AαH) and amphipathic β strand (AβS) structures, respectively, and are believed to be the major lipid associating motifs of apoB (10-15). On the other hand, the βα1 superdomain encompassing the N-terminal up to B22 (residues 1-1000), contains both α-helix and β-sheet structure and is predicted to have a globular, multidomain structure (10). The assembly of nascent lipoprotein particles happens cotranslationally in the ER, i.e. when the N-terminal of apoB is folded with lipids to form a precursor lipoprotein, the C-terminal is still being synthesized by the ribosome (16-18). Moreover, microsomal triglyceride transfer protein (MTP), an essential ER-localized cofactor is required in lipoprotein assembly (19,20). Two MTP binding sites are present in the N-terminal βα1 domain, residues 1-300 and 430-570 (21,22). Further evidence shows that loss of the disulfide bonds in the N-terminal abolishes secretion out of the cell (23-25). Thus the N-terminal sequence is responsible for initiating lipid recruitment and proper folding of the ba1 domain is critical in lipoprotein assembly and secretion.

Dashti et al. showed (26) that in McA-RH7777 cells B22 (the first 1000 amino acids) are necessary for the formation of a nascent lipoprotein particle containing both TAG and phospholipids. Alternatively, Shellness et al. used apoB/MTP transfected COS cells (27) to show that B19.5 (the first 884 amino acids) is capable of forming some lipoproteins. B17 (the first 782 amino acids) secreted from MTP-deficient C127 cells contains a very small amount of surface lipid (28). However B17 binds to dimyristoylphosphatidylcholine (DMPC) (27, 28), phospholipid-TAG emulsions (29) and TAG droplets (30) in vitro. B19 and B20.1 also bind to TAG droplets (31). Thus the N-terminal 22% of apoB contains lipid associating domains and has the required elements to form a primordial lipoprotein particle, and under certain conditions shorter constructs are also adequate (27).

Sequence alignment and analysis show that the βα1 domain is homologous in sequence and amphipathic motifs with lipovitellin (LV) (21,32-36). LV is an ancient lipid transport and storage protein that delivers lipids into oocytes and appears to be a putative ancestor protein of apoB (36,37). The crystal structure of Lamprey LV has been solved at 2.8Å resolution (32). It is comprised of a globular β-barrel domain (also called the N-sheet domain), an α-helical domain and a lipid binding pocket which is lined up by two anti-parallel β-sheet domains (the C-sheet and α-sheet). Based on the structure of LV, homologous models for the N-terminal domain of apoB have been built. Mann et al. (21) modeled the first 587 amino acid of apoB and showed that the homologous β-barrel domain and the central helical domain are conserved. Segrest et al. (33) modeled the whole βα1 domain and showed that it contains domains homologous to the β-barrel, α-helix and two β-sheet domains and proposed a lipid pocket model for the initiation of the lipoprotein particle assembly.

Limited proteolysis results show that the β-barrel, α-helix and the C-sheet domains are three independently folded domains in apoB containing secondary structures consistent with the B20.5 model (Fig. 1) (35,38). Lipid binding experiments show that B5.9 does not bind phospholipids, while B6.4-13 and B13-17 have hydrophobic interfaces which interact with DMPC to form discoidal particles (38). Other fragments of apoB such as B6.4-9, B13-15,

B6.4-15 and B6.4-17 bind phospholipids as well. Thus, B17 contains lipid binding structures that could bind lipids during, or immediately after translocation to initiate the lipoprotein assembly.

Oil-drop tensiometry has been used to study the lipid binding of apolipoproteins and consensus peptides at a TAG/water interface (13,30,31,39-44). It measures the surface behaviors in terms of surface adsorption, desorption, re-adsorption and elastic properties to yield information about lipid-protein interactions. In a previous study, Mitsche, et. al. (44) studied the surface behavior of B6.4-17 which contains both the α-helical (B6.4-13) and the β-sheet domains (B13-17) of apoB. B6.4-17 binds to a TAG/water interface and cannot be completely ejected once bound. However, part of the peptide is pushed off the surface if compressed above 16.7mN/m (Π_{MAX}) and very rapidly snaps back on upon re-expansion. The authors suggested that the N-terminal 8 or 9 helices (B6.4-9) are the structures being pushed off above 16.7mN/m while B13-17 remains bound even at high pressures. Thus, this peptide exhibits properties of both α and β structure and retains some globular structure at the hydrophobic interface. In the present work, we used a similar approach to study the helical (B6.4-13) and sheet (B13-17) domains individually to test the lipid associating ability of these domains and determine the mechanism of lipid-protein interaction.

Experimental procedures

Materials

Two apoB fragments encompassing residues 292-593 (B6.4-13), and 611-782 (B13-17) were expressed from pET24a vectors (Novagen) in BL21 DE3 *E. coli* cells, and purified as described previously (35). Both peptides contain a 6-His tag at the carboxyl terminus. Before interfacial tension studies, B6.4-13 was desalted to 10 mM sodium phosphate/100 mM sodium chloride buffer at pH 7.4 using a PD-10 desalting column (GE biosciences, Pittsburgh, PA) and B13-17 was extensively dialyzed against 5 mM sodium phosphate buffer at pH 7.4. Freshly made B6.4-13 and B13-17 were divided into small aliquots, rapidly frozen in liquid nitrogen and stored at −80 °C. Each peptide aliquot was thawed right before the experiment and discarded afterwards. The concentrations of peptide stocks were determined by Lowry protein assay (45).

Triolein (>99% pure) was purchased from NU-CHEK PREP, INC. (Elysian, MN) and its interfacial tension against buffer is 32 mN/m. All other reagents are of analytical grade. KCl was heated to 600°C for 6 h to remove all organic contaminants before use (41).

Interfacial tension (γ) measurements

The interfacial tension of the triolein/water (TO/W) interface in the presence of different amounts of B6.4-13 or B13-17 in the aqueous phase was measured with an I. T. CONCEPT Tracker oil-drop tensiometer (Longessaigne, France) (46). Peptide stocks were added to the aqueous phase (2 mM pH 7.4 phosphate buffer) to obtain different peptide concentrations from 1.9×10^{-8}M to 2×10^{-7}M for B6.4-13 and from 7.5×10^{-8}M to 3×10^{-7}M for B13-17. A 16 μL triolein drop was formed in the aqueous phase and the interfacial tension (γ) was recorded continuously until it approached an equilibrium level. The surface pressure, Π, is the γ of the interface without peptide (γ_{TO}=32 mN/m) minus γ of the interface with peptide (γ_{pep}), i.e. $\Pi = \gamma_{TO} - \gamma_{pep}$. All experiments were carried out at 25 ± 0.1°C in a thermostated system.

Instantaneous compression and expansion of the interface

To study the desorption and re-adsorption behavior of bound peptides at the interface, near-instant compression and expansion experiments were carried out. Once γ approached an equilibrium level, the oil drop (16 μL) was compressed by suddenly decreasing the volume at

different ratios (6% to 75%). The compressed volume was held for several minutes and then was increased back to the original volume and held for several minutes until γ re-equilibrated. The sudden decrease in drop volume (V) instantaneously decreases the drop surface area (A) and results in a sudden compression causing γ to drop abruptly to a certain level, γ_0. The surface pressure generated is: $\Pi_0 = \gamma_{TO} - \gamma_0$, where γ_{TO} is the surface tension of pure triolein (32 mN/m). If bound peptide or regions of the peptide, desorbs from the surface γ will rise towards an equilibrium value (desorption curve). If the peptide does not desorb, then, the γ will remain essentially constant at the same low level. On re-expansion, free peptide molecules in the aqueous phase or regions of the peptide being ejected from the surface can re-adsorb onto the newly formed surface and γ will fall back to the equilibrium (re-adsorption curve). If the re-adsorption curve (dγ/dt) is the same as the original adsorption curve then we conclude that the entire peptide is ejected from the surface. If however, dγ/dt is much faster, then only part of the peptide is pushed off at compression and snaps back very rapidly when the area is re-expanded (40).

Determination of the Π_{MAX} values

To estimate the maximum pressure (Π_{MAX}) that a peptide can withstand without being fully or partly ejected from the interface, a series of instantaneous compression and re-expansion experiments using different changes in surface area and over a wide range of peptide concentrations were carried out. The tension change, Δγ, over the compression period was plotted against the instant pressure generated right after the compression, Π_0. Then the data was fitted to a straight-line. The intercept at Δγ=0 gives the Π at which the peptide molecules show no net adsorption or desorption, this is Π_{MAX} (40,41).

Oscillation of the interface and the elasticity analysis

Oscillations were carried out after the equilibrium γ (γ_e) was reached. The drop volume (16 μL) was sinusoidally oscillated at varied amplitudes (6%-50% change in volume) and periods (8 to 128 sec). The changes in area (A) and γ were followed as the volume (V) oscillated. In the elasticity analysis, the interfacial elasticity modulus, ε ($\varepsilon = d\gamma/d \ln A$), the phase angle, φ, between the compression and the expansion, the elasticity real part, ε′, and the elasticity imaginary part, ε″, were obtained ($\varepsilon' = |\varepsilon|\cos\varphi$, $\varepsilon'' = |\varepsilon|\sin\varphi$) (47,48).

Buffer exchange procedure

With the surface tension at equilibrium (γ_e), the aqueous phase buffer (6 mL) containing the peptide was exchanged for buffer without peptide using the protocol described previously (39,44). The aqueous phase was continuously removed from the aqueous surface and the new buffer was continuously infused near the bottom of the stirred cuvette. At least ~150 mL buffer was exchanged. If peptide desorbs into the aqueous phase during or after buffer exchange, the surface concentration of peptide will fall and γ will rise.

The instant compression and expansion experiments and the oscillation experiments were also carried out after buffer exchange and compared with that before buffer exchange. Three basically different behaviors are possible. First, if bound peptide is pushed off the surface during compression, then on re-expansion γ will rise to a higher level and stay there since there is virtually no peptide available in the aqueous phase to adsorb back onto the newly formed surface. Second, if only part of the peptide molecule is pushed off the surface on compression, then on re-expansion γ will fall rapidly back to the same equilibrium level since the ejected part of peptide re-adsorbs back on the surface. Finally, compression may cause a conformational change in the peptide which sequesters part of it from the surface and the sequestered part only very slowly re-binds to the surface after re-expansion to lower γ back to the equilibrium level (39).

Langmuir balance studies at the Air/Water (A/W) interface

A solution of each peptide in 30% w/v isopropanol/2 mM phosphate buffer (pH 7.4) was spread slowly (~50 μL/min) on a clean surface of a 3.5 M KCl, 10 mM pH 7.4 phosphate buffer on a KSV 5000 mini trough of a Langmuir/Pockles surface balance (Helsinki, Finland) at 25°C, according to the techniques of Phillips and Krebs (49). Then the surface was compressed at a rate of 5 mN/m/min and the Π-A curves for the peptide monolayer were obtained. To check the reversibility of the Π/A isotherms the peptide monolayer was compressed to a certain Π then re-expanded to a Π lower than 1 mN/m at a rate of 5 mN/m/min, and the compression and expansion curves were compared. The state of the peptide monolayer (liquid, condensed viscous or solid phase) was detected by putting talc powder on the surface, directing a fine jet of air and directly observing the motion of talc particles (50,51). In the liquid state the talc particles move rapidly and freely, in the condensed viscous state they move slowly and in the solid state they are nearly stationary.

Results

Both B6.4-13 and B13-17 are surface active and bind to TO/W interface

The equilibrium interfacial tension of TO/W interface was measured with different amount of peptides present in the aqueous phase. Fig.2A and Fig. 2B are examples of interfacial tension-time curves of B6.4-13 and B13-17. Both peptides are surface active and lower the surface tension (γ) of the TO/W interface (32mN/m) to reach an equilibrium level. The equilibrium γ is dependent on the peptide concentration in the aqueous phase. In general, the higher the peptide concentration the lower the equilibrium γ, and the less time it takes to reach the equilibrium. The γ of the TO/W interface (32mN/m) is lowered to 14.1mN/m with 1.5×10^{-7}M B6.4-13 in the aqueous phase, and 12.6mN/m with B13-17 at the same concentration. Thus, at similar concentrations, B13-17 decreases γ 1.5mN/m more than B6.4-13 indicating that B13-17 has a higher affinity for the TO/W interface.

B6.4-13 only partially desorbs from the TO/W interface on compression and cannot be washed off the interface

Fig. 3A shows an example of tension and area changes during the sudden compression and expansion of the interface for B6.4-13 before and after buffer exchange. The concentration of B6.4-13 in the aqueous phase is 1.9×10^{-7}M before buffer exchange, and the original volume of the triolein drop is 16μl. As the figure shows, after γ approaches an equilibrium level (~13.3mN/m), the drop is compressed by decreasing the volume by 1μL, 2μL, 4μL, 8μL, 10μL and 12μL, respectively. The actual volume changes varied from 5% to 66% and the corresponding area changes varied from 3% to 51%. Every instant compression makes γ fall but then γ rapidly rises towards an equilibrium value while the compressed volume is held for several minutes. The drop is then re-expanded back to 16μl after each compression. Each expansion makes the γ increase above γ_e initially. However, γ returnes back to the equilibrium value (13.4±0.1mN/m) over time. Smaller compressions induces a smaller fall in γ while larger compression induces a greater fall in γ. For example, at 1μL compression, γ droppes from 13.3 to 12.1mN/m and then rises back to 12.8mN/m; at the following expansion, γ rises to 14.1mN/m and then relaxes back to the equilibrium (13.3mN/m). While at 12μL compression, the tension droppes from 13.6mN/m to 3.1mN/m and then rises back to 9.0mN/m; at the following expansion, γ rises to 17.5mN/m and then relaxes back to the equilibrium (13.5mN/m). After every compression γ decreases first and then rises to a new equilibrium level indicating that some material desorbes from the surface on instant compression.

The instant compression and expansion protocol is repeated after buffer exchange (Fig. 3A, right) to find out whether the whole molecule or only some part of the bound B6.4-13 desorbes from the TO/W interface during compression. The buffer exchange procedure is started at 7300

sec when γ is at the equilibrium level and stops at 10300 sec (shown by the bar in Fig. 3A). About 150 mL buffer is exchanged and the concentration of B6.4-13 in the aqueous phase reduces to virtually 0. During the buffer exchange γ remaines the same equilibrium value (13.5 ±0.1mN/m) which indicates that bound B6.4-13 does not desorb from the interface. Then the instant compression and expansion procedure is applied to the triolein drop again (Fig. 3A, right) like that before the buffer exchange (Fig. 3A, left). The changes in γ upon compression/ expansion are very similar to that before the buffer exchange. The γ falls to the similar level on compression, rises to the similar level and then relaxes back to the similar equilibrium level after re-expansion. These data clearly show that only some part of the peptide is pushed off the interface by compression. If the whole peptide molecule is ejected from the interface on compression then γ will remain high after re-expansion because there are virtually no peptide molecules in the aqueous phase available to re-adsorb onto the surface.

Furthermore, the re-adsorption curves at each corresponding expansion, before and after the buffer exchange, are very similar indicating that the re-adsorption is not dependent on the peptide concentration in the aqueous phase. The ejected part of the bound peptide re-adsorbed covering the newly generated surface so quickly that free peptide cannot adsorb onto the surface from the aqueous phase. This data further confirms that only part of the B6.4-13 can be pushed off the surface. However, before or after the buffer exchange, upon compression, the γ always equilibrate to a level lower than the value before compression indicating that the remaining part of the peptide can stand compression and stays compressed to some extent. The fact that the area can be reduced 51% and on re-expansion the γ returns to equilibrium suggests that about ½ of the peptide is pushed off the surface in a form that can rapidly rebind.

B13-17 only partially desorbs from the TO/W interface on compression and cannot be washed off the interface

Fig. 3B shows an example of tension and area changes during the instant compression and expansion of the interface for B13-17 before (2.1×10^{-7}M in the aqueous phase) and after the buffer exchange. γ changes in a very different way from that of B6.4-13. There are three kinds of changes in γ during the compression and re-expansion of the oil droplet at different ratios before the buffer exchange (Fig. 3B, left), shown as 1, 2 and 3 in Fig. 3B. (1) At smaller compressions, (e.g. 1μL volume decrease), γ drops from the equilibrium value 12.2mN/m to 11.6mN/m. γ remains constant when the compressed volume is held. Upon re-expansion, γ rises to 12.4mN/m and quickly equilibrate back to the original value of 12.2mN/m. No desorption is observed. This indicates that no B13-17 is pushed off the surface and bound B13-17 is simply compressed at the surface. (2) At intermediate compression, (e.g. 2, 4 or 8 μL volume decrease), γ falls much further and quickly rises (0.5-1.5mN/m) when the compressed volumes are held. At each following re-expansion, γ rises to a level higher than the original equilibrium value of 12.2mN/m and then relaxes back towards the equilibrium. Thus, at these intermediate compressions, part of the peptide (about 25%) is pushed off the interface but snaps back very quickly upon re-expansion. (3) At bigger compressions, (e.g. 10 and 12μL volume decrease), γ falls deeper but rises back very little. The desorption is slow compared to those in the intermediate compressions. At the following re-expansion, γ rises high and falls back rapidly to levels higher than the equilibrium. We suggest that at these bigger compressions, part of the peptide is pushed off the surface causing conformational changes in a fraction of the peptide which can't re-spread rapidly. After re-expansion, the ejected region of the peptide needs a much longer time to re-arrange its conformation to re-adsorb onto the surface. This results in a very slow change (hours) in γ towards the equilibrium level. Similar behavior is observed with the AβS domain B37-41 (39).

In contrast with B6.4-13, the desorption curves for B13-17 upon compressions bigger than 1 μL has only a slightly smaller increase in γ while the compressed volume is held. For instance

at the 8μL compression (about 30% change in the area), the γ falls from the equilibrium to 4.9mN/m and only rises back to 6.2mN/m, that is a 1.3mN/m tension increase and is very small compare to the tension increase at 8μL expansion of B6.4-13 which is 5.0mN/m (dropped to 5.0mN/m and rises back to 10mN/m). This indicates that there is only a little net desorption of B13-17 at bigger compression, most part of the peptide stayes compressed on the surface.

A buffer exchange is run (shown as the bar in Fig. 3B) to remove B13-17 in the aqueous phase. Similar to that of B6.4-13, γ remaines the same during buffer exchange indicating that no bound peptide desorbes from the interface. Instant compression and expansion measurements are carried out (Fig. 3B, right) using the same protocol as before the buffer exchange (Fig. 3A, left). The same there kinds of changes in the desorption and re-adsorption curves are observed as before the buffer exchange. Therefore only a small part of B13-17 is pushed off the surface upon compression and the majority of B13-17 remains on the surface. If highly compressed the ejected region forms a conformation which is slow to re-spread.

Π_{MAX} values for both B6.4-13 and B13-17

Instant compression followed by re-expansion measurements were carried out at varied peptide concentrations to estimate the Π_{MAX} values for both peptides. Fig. 4 shows that Π_{MAX} of B6.4-13 is 16.7mN/m and Π_{MAX} of B13-17 is 19.2mN/m. The data points shown are a mixture of points taken from the compression and expansion experiments before or after buffer exchange. For both peptides, the whole peptide molecule is not pushed off the surface at our study pressures, so the Π_{MAX} values shown here are the pressures at which parts of the peptides are ejected. A higher Π is needed to push off the ejected region of B13-17 from the interface indicating that the ejected region of B13-17 binds to the TO/W interface more tightly than the ejected region of B6-13. In addition, $\Delta\gamma$ is always much bigger for B6.4-13 than B13-17 at the same pressure indicating that more structure of B6.4-13 tends to desorb from the interface while more structure of B13-17 tends to stay. As a matter of fact, both B6.4-13 and B13-17 can stand a very high surface pressure, e.g. 29mN/m (Fig. 3A and Fig. 3B) at a large compression, e.g. 12 μL (~50% decrease in area), indicating that both peptides have structures that bind strongly to the TO/W interface.

B13-17 is almost purely elastic while B6.4-13 has viscous component on the TO/W interface

Equilibrium oscillations of B6.4-13 and B13-17 at different amplitudes and periods were carried out before and after buffer exchange. These compressions differ from the instantaneous compressions in that they are slow, steady, sinusoidal compressions that are performed at set of rates. Two sets of the surface pressure-area (Π-A) curves for B6.4-13 and B13-17 (all at 1.5×10^{-7}M in the aqueous phase) derived from the oscillations before the buffer exchange are shown in Fig. 5A and Fig. 5B. The Π-A curves for B6.4-13 show significant hysteresis between compression and expansion. The corresponding phase angles, φ, are relatively larger, up to 30° (data not shown) indicating a visco-elastic surface. On the other hand, the Π-A curves for B13-17 show little hysteresis and the phase angles are relatively small, less than 10° (data not shown) indicating a pure elastic surface. There is very little desorption and re-adsorption of the B13-17 during these oscillations. This is further evidence that only a small region of B13-17 desorbs and re-adsorbs. We did series study on the elasticity for both peptides over a wide range of peptide concentration, oscillation amplitude, and oscillation period (data not shown). The φ values average over all experimental conditions for B6.4-13 is 16.6±7.7° and for B13-17 is 4.5±3.8°, indicating that B6.4-13 forms a visco-elastic surface on TO/W interface while B13-17 is mainly elastic. Between the two peptides, B13-17 has a higher modulus (38±7.3mN/m) than B6.4-13 (25.6±6.5mN/m). The elasticity modulus is the increase in the surface tension for a small increase in area of a surface element ($\varepsilon = d\gamma / d \ln A$), is the mathematical description of the surface's tendency to be deformed elastically (i.e., non-permanently) when a force is applied to it. A higher elasticity modulus indicates a more rigid molecule. This is consistent

with the larger phase angles for B6.4-13 relative to B13-17. In other words, B13-17 is more rigid and less compressible than B6.4-13.

Examples for the elasticity modulus, ε, from the oscillations before and after buffer exchange are compared for both peptides in Fig. 6. Similar results are present either before or after the buffer exchange at the same peptide, same amplitude and same period. ONE-WAY ANOVA analysis at 0.05 level showes that the ε, φ and ε' of corresponding oscillations are not significantly different before and after buffer exchange (data not shown). This indicates that there is no whole molecule desorption from the interface or re-adsorption onto the interface.

Monolayers of B6.4-13 and B13-17 at the A/W interface

Fig. 7 shows the pressure/area (Π-A) isotherms for B6.4-13 and B13-17. The limiting area for B6.4-13 is 16.6 $Å^2$/aa and the B6.4-13 monolayer collapses at 31 mN/m at the area of 12.2 $Å^2$/aa. The limiting area for B13-17 is 17.8 $Å^2$/aa and the B13-17 monolayer collapses at 35 mN/m at the area of 13.3 $Å^2$/aa. Both B6.4-13 and B13-17 can be reversibly compressed and expanded at pressures below the collapse pressure (31mN/m and 35mN/m), respectively (data not shown). By observing the movement of the Talc powder on the surface, we found that B13-17 monolayer starts solidify right after the lift up (Π>2mN/m) which is typical for a β sheet structure (39). In contrast, the B6.4-13 monolayer does not solidify until Π is over 10mN/m and becomes solid when Π reaches 20 mN/m. The average area per residue for proteins adsorbed flat on a surface is 15-25 $Å^2$/aa, so both peptides are likely flat at the A/W interface.

Discussion

When proteins or peptides come to hydrophobic interfaces like oil/water or air/water (A/W) interfaces, different structures behave differently. When some water soluble globular proteins adsorbs to the hydrophobic interface, since they hide most of their hydrophobic residues in the core of the molecule, they undergo major conformational changes after binding and denature to gradually decrease the interfacial tension (47,52). On the contrary, apolipoproteins are specifically evolved for lipid binding with the characteristic secondary structures of AαH and AβS (10-14). When approaching a hydrophobic interface, they don't denature, instead they rapidly adsorb and retain the secondary structures.

AαH and AβS structures show characteristic interfacial properties at TO/W interface in terms of the adsorption, the desorption and re-adsorption, the elasticity and the compressibility. Both AαH and AβS structures are surface active, they adsorb onto the surface and lower the surface tension rapidly (13,15,40,43). AβS structures show strong irreversible binding to TO/W interface (13,39). They can be compressed to a very high surface pressure (about 28-29 mN/m) and stay compressed without leaving the surface. Bound AβS structures display purely elastic properties with very small phase angles at the surface when the surface area changes less than 15% (13). When applied to an A/W interface on a monolayer trough, AβS structures quickly interact with each other when compressed to a low pressure and form solid monolayer suggesting a large extended β sheet structure at very low pressure (1 to 2 mN/m) (39). This large β sheet can be compressed and expanded reversibly up to its collapse pressure (usually around or higher than 35mN/m) (39 and unpublished data). AαH structures show reversible binding to TO/W surface. In general they desorb from the surface when the surface is compressed above 13-19mN/m (15,40,42) and re-adsorb quickly when the surface is re-expanded. This reversible on and off behavior of AαH was proposed in the review by Segrest, et al. (10). Some AαH structures with lower surface affinity, like the N-terminal domain of apoA-I (residue 1-44), can partially desorb from the surface without compression during exchanging the peptide out of the aqueous phase (43 and unpublished data). AαH show purely elastic properties only at smaller changes in the surface area and at fast rates, otherwise they are visco-elastic at the surface (15,40,42). When applied to an A/W interface, AαH structure

does not become a solid monolayer until the pressure reaches well above 10 mN/m. As observed for AβS, AαH monolayer can also be reversibly compressed and expanded as long as the pressure remains below the collapse pressure.

According to the LV homology model of B17, B6.4-13 and B13-17 are distinct domains containing α and β structures with amphipathic features (35,38, and Fig. 8). Our study show that B6.4-13 binds to TO/W interface (Fig. 2A) but unlike most AαH, cannot be completely pushed off the TO/W interface (Fig. 3A). B6.4-13 does show typical partial desorption and re-adsorption curves of AαH structures, i.e. fast desorption at compression and fast re-adsorption at re-expansion towards the equilibrium. This indicates that the majority of the secondary structure of this domain is AαH. This is consistent with the model prediction and the CD spectra that show nearly 60% its secondary structure is α helix in B6.4-13 (35). Up to 50% of B6.4-13 desorbs from the TO/W interface at pressures above 16.7 mN/m (Fig. 4). This is within the Π_{MAX} range for the AαH structures in exchangeable apolipoproteins (13-19 mN/m) and is consistent with the Π_{MAX} value of B6.4-17 (16.7 mN/m) (44). Thus, when B6.4-17 is compressed at the interface, regions in the B6.4-13 domain are pushed off at lower pressures than B13-17. The B13-17 domain has a higher lipid binding affinity with a Π_{MAX} of 19.2 mN/m (Fig. 4), but most of the peptide remains bound, is elastic and cannot desorb. B6.4-13 has visco-elastic properties at the TO/W interface like other AαH structures in the exchangeable apolipoproteins as well. At an A/W interface, the limiting area for B6.4-13 monolayer is 16.6 $Å^2$ per residue and the collapse pressure is 31 mN/m indicating that the peptide is lying flat on the surface (Fig. 7).

That B6.4-13 cannot be pushed off the interface is a little surprising because all other AαH structures (apoA-I, apoA-I fragments and the consensus peptides) we have studied can be pushed off the interface by compression (15,40,42). We note that some of the α helix structures in B6.4-13 domain are not those classic type A or type Y AαH found in exchangeable apolipoproteins or in the α2 or α3 domains of apoB (Fig. 8). Some of the α-helixes are very hydrophobic without a clear hydrophilic face, e.g. helices 5, 6 and 8. These helices are more similar to transmembrane α-helices, but shorter. We speculate that they may fully insert into the hydrophobic lipid and then cannot be pushed off by compression. Helices 5, 6 and 8 face the lipid pocket in the B17 model (Fig. 8), especially helix 6 and 8 that bind to the lipid directly in the LV structure. Some helices in the C-terminal of B6.4-13 are typical for globular proteins and have a lot of charged residues. They do not show strong lipid binding affinity for DMPC (38). In the LV homology model, those charged residues interact with the charged side of the β sheet formed by B13-17 domain. Mitsche, et. al. (44) have studied the interfacial properties of B6.4-17 which encompasses both the α-helical domain (B6.4-13) and the β-sheet domain (B13-17) at TO/W and A/W interfaces. Only about 60% of the expected area of B6.4-17 binds to the A/W interface. The authors suggest that the C-terminal part of the helical domain (B9-13) retains protein-protein interactions with the hydrophilic face of the β sheet domain and thus does not contact the surface. In our study, lacking protein-protein interactions with B13-17, those C-terminal helices of B6.4-13 with charged residues might partially denature like a globular structure and irreversibly bind to the hydrophobic interface. That is another possible reason for B6.4-13 not being fully pushed off by compression.

B13-17 showes strong binding to the TO/W interface (Fig. 2B). It has a very high Π_{MAX} value of 19.2 mN/m (Fig. 4) and is almost purely elastic (Fig. 5B). B13-17 cannot be washed off or pushed off the interface (Fig. 3B). Only a small region of the sequence can be pushed off the interface by compression as shown by the very small increase in the surface tension after compression (Fig. 3B). This is the typical desorption behavior of AβS structures (13,39), and is consistent with the model which predicts that B13-17 contains 6 anti-parallel β strands forming a β sheet (Fig. 8). The re-adsorption curves of B13-17 at intermediate compression shows a very rapid fall back to the equilibrium level (Fig. 3B), and at larger compression, the

re-adsorption curves return to near the equilibrium values, and there is no significant difference after the buffer exchange. Together, this suggests that only a small region of B13-17 is pushed off the surface and re-adsorbed rapidly.

We notice that at larger compression, the re-adsorption curves do not fall back to the equilibrium level (different by 1-2mN/m). We have shown similar phenomena in our study of B37-41, a large AβS structure (39). When B37-41 is compressed by 36% and then re-expanded γ rises to 23.9 mN/m then relaxes back in 40 min to 22.7 mN/m (6.5 mN/m higher than the equilibrium, e.g. 16.2 mN/m). Then after ~12 hours, the tension gradually fell back to 19.7 mN/m. We suggest that larger compression causes some conformational changes of the ejected region that requires more time to return to the equilibrium. In the LV homology model of B20.5 (Fig. 1), a large loop of amino acids (656-729) between strands 4 and 5 of the β-sheet in B13-17 is missing because this part is not present in the LV structure. This region has been predicted to contain an AαH structure (33). CD study shows 30.7% of a content in B13-17 (35). Those helical structures might be the region that leaves the surface upon compression and re-adsorbs at expansion.

Thus, both B6.4-13 and B13-17 display strong lipid binding to TO/W interface. Both of them contain structures irreversibly bind to lipid. B13-17 has a higher affinity and is more elastic than B6.4-13. They show typical surface behaviors of AαH and AβS structures suggesting that the main secondary structures of the two domains are α-helix and β-sheet respectively, which are consistent with the homologous B17 model and with the surface study of B6.4-17 (Table 1) (35,38,44).

There are two competing models for the initiation of apoB lipoprotein assembly. A lipid pocket model is proposed that the N-terminal 1000-residues βα1 domain of apoB forms a lipid pocket homologous to that of lamprey lipovitellin during translation, which contains two β sheet connected by a central α-helical domain and a helix-turn-helix motif close the pocket (53). This pocket is gradually filled with phospholipids and converted to a nascent TAG-core emulsion particle as the translation continuous. While the βα1 domain contains the required sequence and structural elements for initiating assembly, the amino acid residues between 931 and 1000 maybe critical for the formation of a stable, bulk-lipid containing nascent lipoprotein particle (53). In an alternative “intercalation/desorption model”, the two sides of the lipovitellin-like cavity form solvent-accessible surfaces with strong interfacial binding properties interact with the ER membrane to sequester neutral lipids to nucleate the oil droplet formation and ultimately desorbs from the membrane as a small neutral lipid core-containing precursor particle (27). The suggestion that B19.5 is secreted in a small particle with a neutral lipid core (27) and that B17, B19 and B20.1 bind to a TAG/W interface (30,31) are used in support of this model. Both models agree that the N-terminal domain contains the structure and required elements for lipid binding. But they differ on the mechanism and what sequence is involved in the lipid binding.

Our study shows that as early as B6.4 in the N-terminal domain of apoB, the structure possesses the ability to bind to neutral lipids. Both B6.4-13 and B13-17 contain the elements that strongly bind lipids. This is consistent with the study showing that B6.4-17, B17, B19 and B20.1 all bind to TAG interface in vitro (30,31,44). In vivo studies show that truncated apoB of different size is secreted with different lipid composition. B17 is secreted with only a small amount of phospholipids (28). B22 and B19.5 are claimed to be the minimum size required for lipoprotein particle assembly and secretion in different cell lines (26,27). We think that the lipid recruitment may start early but only sequences containing a more complete lipid pocket (i.e. B19.5 or B22) can stabilize the emulsion particle and be secreted. B32.5, B37 and B41 are secreted as stable lipoprotein particles containing increasing core lipids (54). So, during apoB translocation, the lipid recruiting may start as early as B6.4 but future sequences as translation continues are required to produce a stable emulsion particle which can be secreted.

In summary, our interfacial studies on the two distinct domains (B6.4-13 and B13-17) in the LV homologous N-terminal domain of apoB show that both domains contain lipid associating structures. The majority secondary structure of the two domains is AαH and AβS respectively, which is consistent with the B20.5 model. The two domains show different surface behaviors at TO/W interface but they work together to form a hydrophobic face to bind to TAG surface.

Acknowledgments

This work is supported in part by Grant NIH-NHLBI 2P01 HL26335-21.

Abbreviations

ApoB	apolipoprotein B
VLDL	very low density lipoprotein
IDL	intermediate density lipoprotein
LDL	low density lipoprotein
TAG	triacylglycerol
B100	the full length of apoB
B48	the N-terminal 48% of apoB
AαH	amphipathic α helix
AβS	amphipathic β strand
MTP	microsomal triglyceride transfer protein
DMPC	dimyristoylphosphatidylcholine
LV	lipovitellin
TO/W	triolein/water
A/W	air/water

References

1. Kane, JP.; Havel, RJ. Disorders of the Biogenesis and Secretion of Lipoproteins Containing the B Apolipoproteins. In: Scriver, CR.; Beaudet, AL.; Sly, WS.; Valle, D., editors. The Metabolic Bases of Inherited Disease. 8th ed.. Medical Publishing Division, USA; McGraw-Hill: 2001. p. 2717-2752.Chapter 115
2. Havel, RJ.; Kane, JP. Introduction: Structure and Metabolism of Plasma Lipoproteins. In: Scriver, CR.; Beaudet, AL.; Sly, WS.; Valle, D., editors. The Metabolic Bases of Inherited Disease. 8th ed.. Medical Publishing Division, USA; McGraw-Hill: 2001. p. 2705-2716.Chapter 114
3. Kane JP. Plasma lipoproteins and their receptors. Curr. Opin. Structural Biol 1991;1:510–515.
4. Chen GC, Liu W, Duchateau P, Allaart J, Hamilton RL, Mendel CM, Lau K, Hardman DA, Frost PH, Malloy MJ. Conformational differences in human apolipoprotein B-100 among subspecies of low density lipoproteins (LDL). Association of altered proteolytic accessibility with decreased receptor binding of LDL subspecies from hypertriglyceridemic subjects. J. Biol. Chem 1994;269:29121–29128. [PubMed: 7961878]
5. McNamara J, Small DM, Li Z, Schaefer EJ. Differences in LDL subspecies involve alterations in lipid composition and conformational changes in apolipoprotein B. J. Lipid Res 1996;37:1924–1935. [PubMed: 8895058]
6. Krauss RM, Burke DJ. Identification of multiple subclasses of plasma low density lipoproteins in normal humans. J. Lipid Res 1982;23:97–104. [PubMed: 7057116]

7. Hurt-Camejo E, Camejo G, Rosengren B, Lopez F, Wiklund O, Bondjers G. Differential uptake of proteoglycan-selected subfractions of low density lipoprotein by human macrophages. J. Lipid Res 1990;8:1387–1398. [PubMed: 2280180]
8. Gantz DL, Walsh MT, Small DM. Morphology of sodium deoxycholate-solubilized apolipoprotein B-100 using negative stain and vitreous ice electron microscopy. J. Lipid Res 2000;41:1464–1472. [PubMed: 10974054]
9. Spin JM, Atkinson D. Cryoelectron microscope of low density lipoprotein in vitreous ice. Biophys. J 1995;68:2115–2123. [PubMed: 7612855]
10. Segrest JP, Jones MK, De Loof H, Dashti N. Structure of apolipoprotein B-100 in low density lipoproteins. J Lipid Res 2001;42:1346–1367. [PubMed: 11518754]
11. Nolte, RT. Structural Analysis of the Human Apolipoproteins: an Integrated Approach Utilizing Physical and Computational Methods. Boston University School of Medicine; Boston: 1994. PhD Thesis
12. Segrest JP, Jones MK, Mishra VK, Anantharamaiah GM, Garber DW. ApoB-100 has a pentapartite structure composed of three amphipathic alpha-helical domains alternating with two amphipathic beta-strand domains. Detection by the computer program LOCATE. Arterioscler. Thromb 1994;14:1674–1685. [PubMed: 7918318]
13. Wang L, Small DM. Interfacial properties of amphipathic β strand consensus peptides of apolipoprotein B at oil/water interfaces. J. Lipid Res 2004;45:1704–1715. [PubMed: 15231853]
14. Small DM, Atkinson D. The first beta sheet region of apoB(apoB21-41) is a amphipathic ribbon 50-60Å wide and 200Å long which initiates triglyceride binding and assembly of nascent lipoproteins. Circulation 1997;96:1.
15. Wang L, Atkinson D, Small DM. Interfacial properties of an amphipathic α-helix consensus peptide of exchangeable apolipoproteins at air/water and oil/water interfaces. J. Biol. Chem 2003;278:37480–37491. [PubMed: 12842901]
16. Pease RJ, Harrison GB, Scott J. Co-translocational insertion of apolipoprotein B into the inner leaflet of the endoplasmic reticulum. Nature 1991;353:448–450. [PubMed: 1896087]
17. Spring DJ, Chen-Liu LW, Chartterton JE, Elovson J, Schumaker VN. Lipoprotein assembly. Apolipoprotein B size determines lipoprotein core circumference. J. Biol. Chem 1992;267:14839–14845. [PubMed: 1321819]
18. Schumaker VN, Phillips ML, Chatterton JE. Apolipoprotein B and low-density lipoprotein structure: Implications for biosynthesis of triglyceride-rich lipoproteins. Adv. Protein Chem 1994;45:205–248. [PubMed: 8154370]
19. Wetterau JR, Aggerbeck LP, Bouma ME, Eisenberg C, Munck A, Hermier M, Schmitz J, Gay G, Rader DJ, Gregg RE. Absence of microsomal triglyceride transfer protein in individuals with abetalipoproteinemia. Science 1992;258:999–1001. [PubMed: 1439810]
20. Wetterau JR, Gregg RE, Harrity TW, Arbeeny C, Cap M, Connolly F, Chu CH, George RJ, Gordon DA, Jamil H, Jolibois KG, Kunselman LK, Lan SJ, Maccagnan TJ, Ricci B, Yan M, Young D, Chen Y, Fryszman OM, Logan JVH, Musial CL, Poss MA, Robl JA, Simpkins LM, Slusarchyk WA, Sulsky R, Taunk P, Magnin DR, Tino JA, Lawrence RM, Dickson JK Jr. Biller SA. An MTP inhibitor that normalizes atherogenic lipoprotein levels in WHHL rabbits. Science 1998;282:751–754. [PubMed: 9784135]
21. Mann CJ, Anderson TA, Read J, Chester SA, Harrison GB, Kochl S, Ritchie PJ, Bradbury P, Hussain FS, Amey J, Vanloo B, Rosseneu M, Infante R, Hancock JM, Levitt DG, Banaszak LJ, Scott J, Shoulders CC. The structure of vitellogenin provides a molecular model for the assembly and secretion of atherogenic lipoproteins. J. Mol. Biol 1999;285:391–408. [PubMed: 9878414]
22. Hussain MM, Bakillah A, Nayak N, Shelness GS. Amino acids 430-570 in apolipoprotein B are critical for its binding to microsomal triglyceride transfer protein. J. Biol. Chem 1998;273:25612–25615. [PubMed: 9748226]
23. Burch WL, Herscovitz H. Disulfide bonds are required for folding and secretion of apolipoprotein B regardless of its lipidation state. J. Biol. Chem 2000;275:16267–16274. [PubMed: 10747912]
24. Huang XF, Shelness GS. Identification of cysteine pairs within the amino-terminal 5% of apolipoprotein B essential for hepatic lipoprotein assembly and secretion. J. Biol. Chem 1997;272:31872–31876. [PubMed: 9395534]

25. Tran K, Boren J, Macri J, Wang Y, McLeod R, Avramoglu RK, Adeli K, Yao Z. Functional analysis of disulfide linkages clustered within the amino terminus of human apolipoprotein B. J. Biol. Chem 1998;273:7244–7251. [PubMed: 9516417]
26. Dashti N, Manchekar M, Liu Y, Sun Z, Segrest JP. Microsomal Triglyceride Transfer Protein Activity Is Not Required for the Initiation of Apolipoprotein B-containing Lipoprotein Assembly in McA-RH7777 Cells. J. Biol. Chem 2007;282:28597–28608. [PubMed: 17690102]
27. Shelness GS, Hou L, Ledford AS, Parks JS, Weinberg RB. Identification of the Lipoprotein Initiating Domain of Apolipoprotein B. J. Biol. Chem 2003;278:44702–44707. [PubMed: 12941937]
28. Herscovitz H, Hadzopoulou-Cladaras M, Walsh MT, Cladaras C, Zannis VI, Small DM. Expression, secretion, and lipid-binding characterization of the N-terminal 17% of apolipoprotein B. Proc Natl. Acad. Sci. U S A 1991;88(16):7313–7317. [PubMed: 1871138]
29. Herscovitz H, Derksen A, Walsh MT, McKnight CJ, Gantz DL, Hadzopoulou-Cladaras M, Zannis V, Curry C, Small DM. The N-terminal 17% of apoB binds tightly and irreversibly to emulsions modeling nascent very low density lipoproteins. J. Lipid Res 2001;42(1):51–59. [PubMed: 11160365]
30. Weinberg RB, Cook VR, DeLozier JA, Shelness GS. Dynamic interfacial properties of human apolipoproteins A-IV and B-17 at the air/water and oil/water interface. J. Lipid Res 2000;41:1419–1427. [PubMed: 10974049]
31. Ledford AS, Cook VA, Shelness GS, Weinberg RB. Structural and dynamic interfacial properties of the lipoprotein initiating domain of apolipoprotein B. J. Lipid Res 2009;50:108–115. [PubMed: 18711207]
32. Anderson TA, Levitt DG, Banaszak LJ. The structural basis of lipid interactions in lipovitellin, a soluble lipoprotein. Structure 1998;6:895–909. [PubMed: 9687371]
33. Segrest JP, Jones MK, Dashti N. N-terminal domain of apolipoprotein B has structural homology to lipovitellin and microsomal triglyceride transfer protein: a “lipid pocket” model for self-assembly of apoB-containing lipoprotein particles. J. Lipid Res 1999;40:1401–1416. [PubMed: 10428976]
34. Read J, Anderson TA, Ritchie PJ, Vanloo B, Amey J, Levitt D, Rosseneu M, Scott J, Shoulders CC. A mechanism of membrane neutral lipid acquisition by the microsomal triglyceride transfer protein. J. Biol. Chem 2000;275:30372–30377. [PubMed: 10893406]
35. Jiang ZG, Carraway M, McKnight CJ. Limited proteolysis and biophysical characterization of the lipovitellin homology region in apolipoprotein B. Biochemistry 2005;44(4):1163–1173. [PubMed: 15667210]
36. Baker ME. Is vitellogenin an ancestor of apolipoprotein B-100 of human low-density lipoprotein and humen lipoprotein lipase. Biochem. J 1988;255:1057–1060. [PubMed: 3145737]
37. Meininger T, Raag R, Roderick S, Banaszak LJ. Preparation of single crystals of a yolk lipoprotein. J. Mol. Biol 1984;179:759–764. [PubMed: 6502715]
38. Jiang ZG, Gantz D, Bullitt E, McKnight CJ. Defining lipid-interacting domains in the N-terminal region of apolipoprotein B. Biochemistry 2006;45(39):11799–11808. [PubMed: 17002280]
39. Wang L, Martin DD, Genter E, Wang J, McLeod RS, Small DM. Surface study of apoB1694-1880 shows this sequence anchors apoB to lipoproteins and makes it nonexchangeable. J. Lipid Res 2009;50:1340–1352. [PubMed: 19251580]
40. Wang L, Atkinson D, Small DM. The interfacial properties of apoA-I and an amphipathic α-helix consensus peptide of exchangeable apolipoproteins at the triolein/water interface. J. Biol. Chem 2005;280:4154–4165. [PubMed: 15695525]
41. Wang L, Walsh MT, Small DM. Apolipoprotein B is conformationally flexible but anchored at a triolein/water interface: a possible model for lipoprotein surfaces. Proc. Natl. Acad. Sci. U.S.A 2006;103:6871–6876. [PubMed: 16636271]
42. Wang L, Hua N, Atkinson D, Small DM. The N-terminal (1-44) and C-terminal (198-243) peptides of apolipoprotein A-I behave differently at the triolein/water interface. Biochemistry 2007;46:12140–12151. [PubMed: 17915945]
43. Small DM, Wang L, Mitsche MA. The adsorption of biological peptides and proteins at the oil/water interface. A potentially important but largely unexplored field. J. Lipid Res 2009;50:S329–S334. [PubMed: 19029067]

44. Mitsche MA, Wang L, Jiang ZG, McKnight CJ, Small DM. Interfacial properties of a complex multi-domain 490 amino acid peptide derived from apolipoprotein B (residues 292-782). Langmuir 2009;25:2322–2330. [PubMed: 19146422]
45. Lowry OH, Rosebrough NJ, Farr AL, Randall RJ. Protein measurement with the Folin phenol reagent. J. Biol. Chem 1951;193:265–275. [PubMed: 14907713]
46. Labourdenne S, Gaudry-Rolland N, Letellier S, Lin M, Cagna A, Esposito G, Verger R, Rivière C. The oil-drop tensiometer: potential applications for studying the kinetics of (phospho)lipase action. Chem. Phys. Lipids 1994;71:163–173.
47. Benjamins, J.; Lucassen-Reynders, EH. Surface Dilational Rheology of Proteins Adsorbed at Air/Water and Oil/Water Interfaces In Proteins at Liquid Interfaces. Möbius, D.; Miller, R., editors. Elsevier; Amsterdam: 1998. p. 341-384.
48. Benjamins J, Cagna A, Lucassen-Reynders EH. Viscoelastic properties of triacylglycerol/water interfaces covered by proteins. Colloids Surf 1996;114:245–254.
49. Phillips MC, Krebs KE. Studies of apolipoproteins at the air-water interface. Methods Enzymol 1986;128:387–403. [PubMed: 3724515]
50. Fahey DA, Small DM. Surface properties of 1, 2-dipalmitoyl-3-acyl-sn-glycerols. Biochemistry 1986;25:4468–4472. [PubMed: 3756148]
51. Fahey DA, Small DM. Phase behavior of monolayers of 1, 2-dipalmitoyl-3-acyl-sn-glycerols. Langmuir 1988;4:589–594.
52. Beverung CJ, Radke CJ, Blanch HW. Protein adsorption at the oil/water interface: characterization of adsorption kinetics by dynamic interfacial tension measurements. Biophys. Chem 1999;81:59–80. [PubMed: 10520251]
53. Richardson PE, Manchekar M, Dashti N, Jones MK, Beigneux A, Young SG, Harvey SC, Segrest JP. Assembly of lipoprotein particles containing apolipoprotein-B: structural model for the nascent lipoprotein particle. Biophys J 2005;88(4):2789–800. [PubMed: 15653747]
54. Carraway M, Herscovitz H, Zannis V, Small DM. Specificity of lipid incorporation is determined by sequences in the N-terminal 37 of apoB. Biochemistry 2000;39:9737–9745. [PubMed: 10933790]

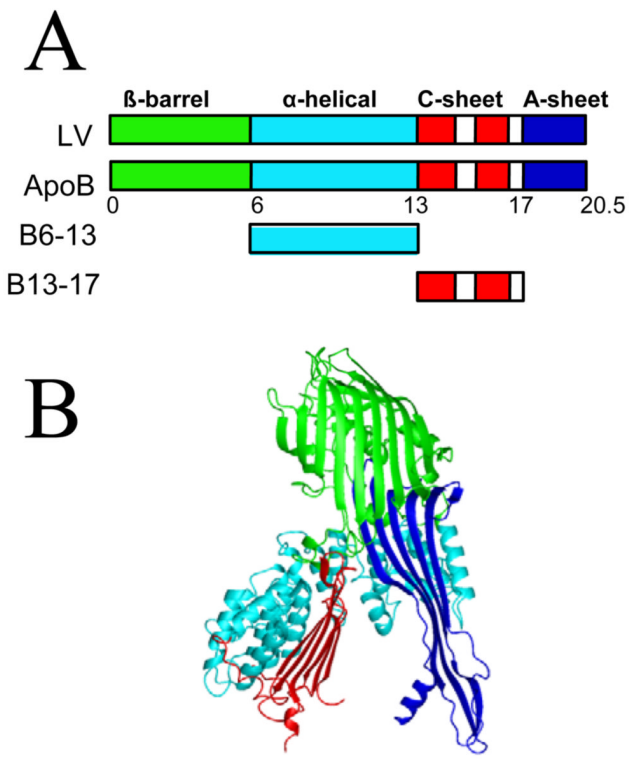

Fig. 1.

Homology model of B20.5. (A) Comparison of domain structures of lipovitellin (LV) and B20.5. Only the N-terminal 20.5% of apoB is colored by proposed domains. β-barrel domain, green; α-helical domain, cyan; C-sheet, red; A-sheet, dark blue; missing regions in the structure of LV, white. (B) Ribbon representation of B20.5 model colored by domain as in panel (A).

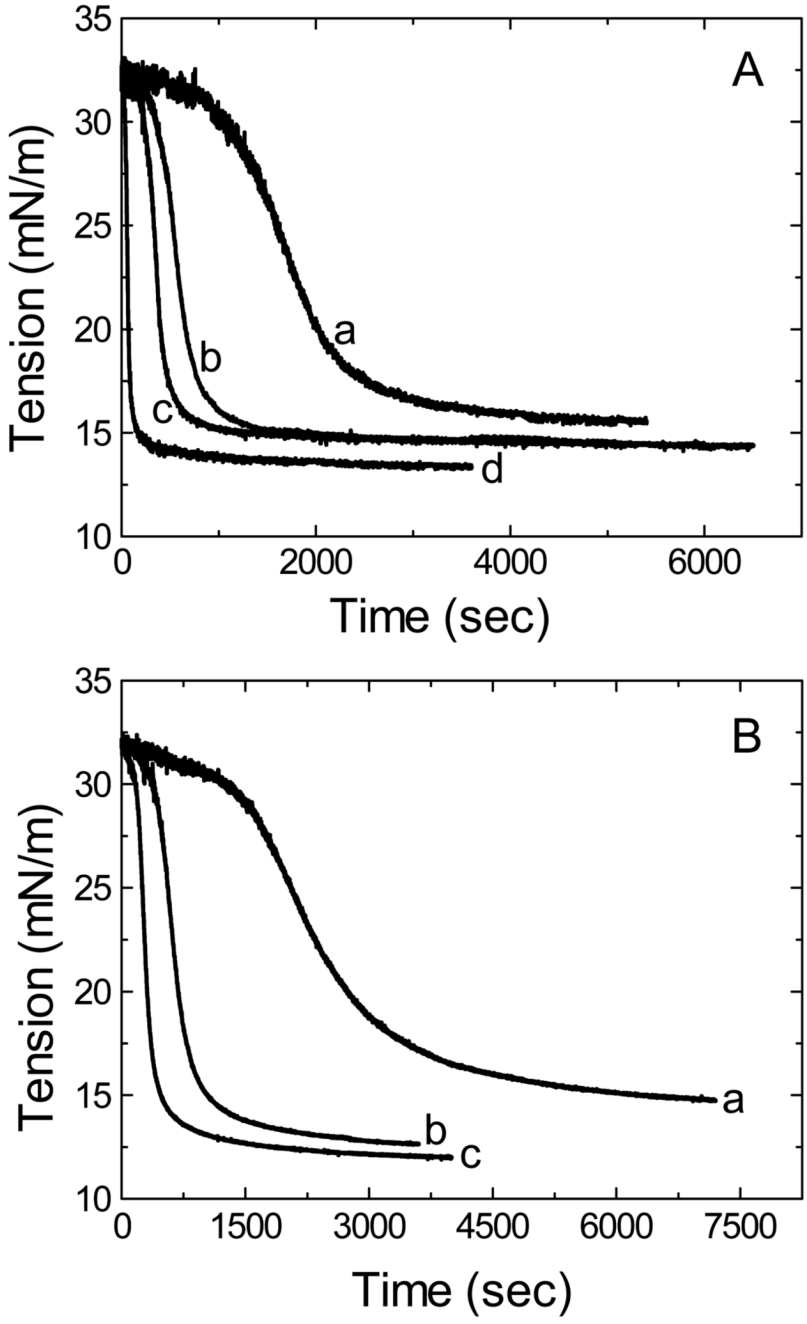

Fig. 2.

Examples of the interfacial tension (γ) versus time curves for B6.4-13 (A) and B13-17 (B) at TO/W interface. A 16 μl triolein drop was formed in 2mM, pH7.4 phosphate buffer with different amounts of peptides. A. The concentration of B6.4-13 in the aqueous phase was (a) 2×10^{-8}M; (b) 3.8×10^{-8}M; (c) 1.5×10^{-7}M; and (d) 2.0×10^{-7}M. B. The concentration of B13-17 in the aqueous phase was (a) 7.5×10^{-8}M; (b) 1.5×10^{-7}M; and (c) 3.0×10^{-7}M. All the measurements were carried out at 25 ± 0.1°C.

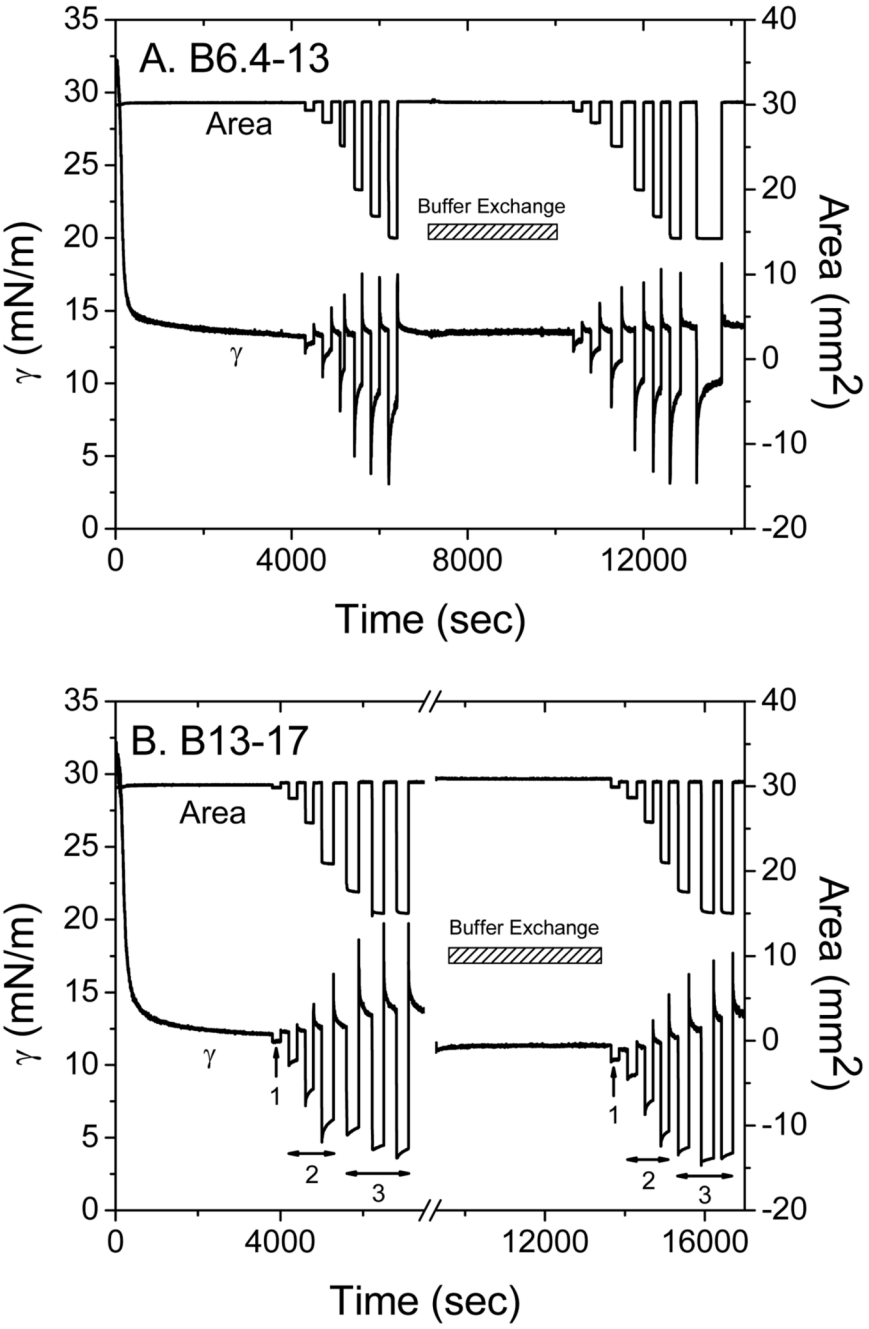

Fig. 3.

Examples of the interfacial tension (γ) and the area versus time curves for B6.4-13 (A) and B13-17 (B) at TO/W interface and the instant compression and re-expansion measurement before and after buffer exchange procedure. (A) The concentration of B6.4-13 in aqueous phase was 1.9×10^{-7} M before the buffer exchange and virtually zero after the buffer exchange. A 16 μl triolein drop was formed in 2 mM pH 7.4 phosphate buffer. After γ reached an equilibrium level, the triolein drop was compressed by decreasing the volume by 1, 2, 4, 8, 10 and 12 μl (corresponding to about 3% to 51% changes in area), and then after several minutes re-expanded back to the original volume 16 μl after each compression. About 150mL buffer was exchanged during the buffer exchange procedure (shown by the bar). After the buffer exchange,

the triolein drop was compressed by decreasing the volume by 1, 2, 4, 8, 10 and 12 μl (×2), and re-expanded back to the original volume 16 μl after each compression. (B) Similar protocol applied to B13-17. The concentration of B13-17 in aqueous phase was 2.1×10^{-7} M before the buffer exchange and virtually zero after the buffer exchange. After γ reached an equilibrium level, the triolein drop was compressed by decreasing the volume by 1, 2, 4, 8, 10 and 12 μl (×2) (corresponding to about 1% to 49% changes in area), and then after several minutes re-expanded back to the original volume 16 μl. About 150mL buffer was exchanged during the buffer exchange procedure (shown by the bar). After the buffer exchange, the triolein drop was compressed by decreasing the volume by 1, 2, 4, 8, 10 and 12 μl (×2), and re-expanded back to the original volume 16 μl. All experiments were carried out at 25 ± 0.1°C.

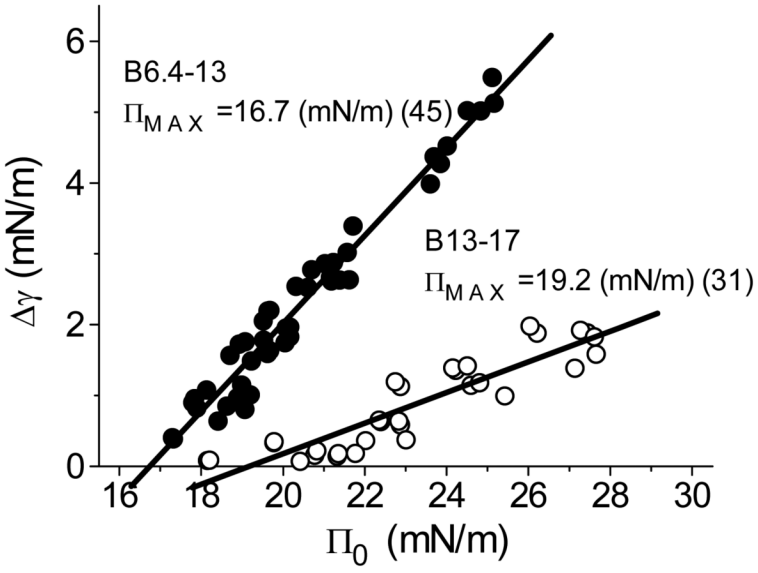

Fig. 4.

Π_{MAx} of B6.4-13 (solid circles) and B13-17 (open circles) at TO/W interface. The interface was instantly compressed to generated pressure Π_0, and the change in the interfacial tension (Δg) while the compressed volume was held for several minutes was plotted against Π_0 and the data were fitted to a straight line. The intercept of the fit lines at $\Delta\gamma$=0 gives Π_{MAx}, the pressure at which peptides shows no net desorption or adsorption. The data points shown are a mixture of points taken from the compression and expansion experiments before or after buffer exchange. The numbers of the data points taken for each peptide are shown in the parentheses.

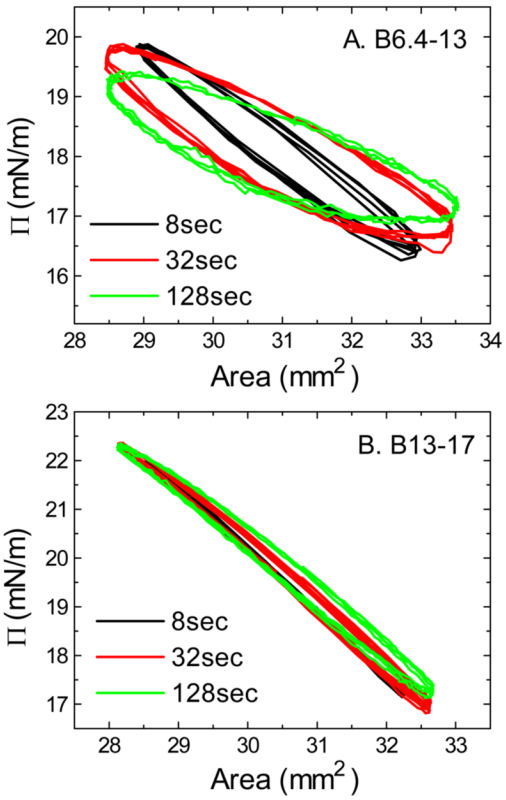

Fig. 5.

Surface pressure (Π) versus area plots of B6.4-13 (A) and B13-17 (B) at TO/W interface derived from oscillations before the buffer exchange procedure. After the equilibrium tension (γ_e) was reached a 16μl triolein drop was oscillated at 16−/+2μl and different periods from 8 to 128sec. (A) The concentration of B6.4-13 in the aqueous phase was 1.5×10^{-7}M. (B) The concentration of B13-17 in the aqueous phase was 1.5×10^{-7}M. All experiments were carried out at 25 ± 0.1°C.

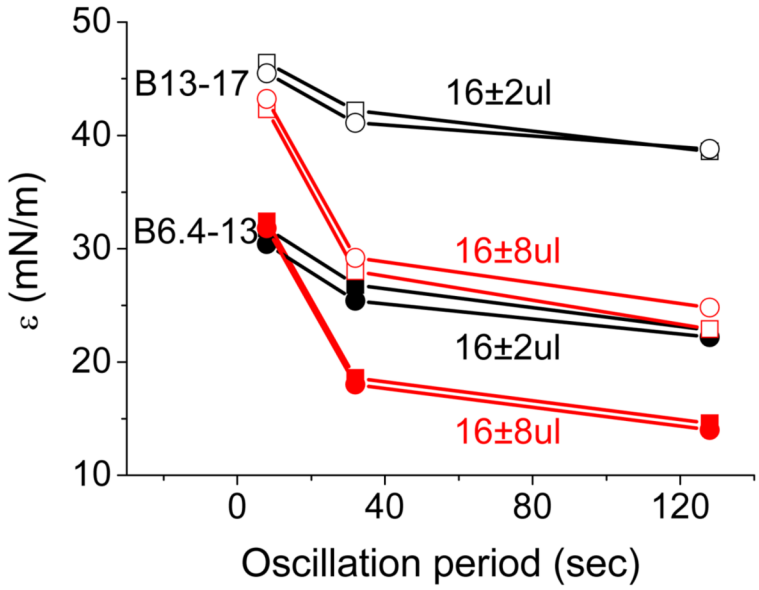

Fig. 6.

Comparison for the changes of the elasticity modulus (ε) as a function of the oscillation period of B6.4-13 and B13-17 at the TO/W interface derived from the oscillations before and after the buffer exchange procedure. The peptide concentration in the aqueous phase before buffer exchange was 2.0×10^{-7}M for B6.4-13 or 2.1×10^{-7}M for B13-17. After buffer exchange, both peptides were absent from the aqueous phase. Solid symbols are for B6.4-13; open symbols are for B13-17; squares are for pre-exchange; circles are for post-exchange; black symbols are for 16±2 μl oscillations; red symbols are for 16±8 μl oscillations.

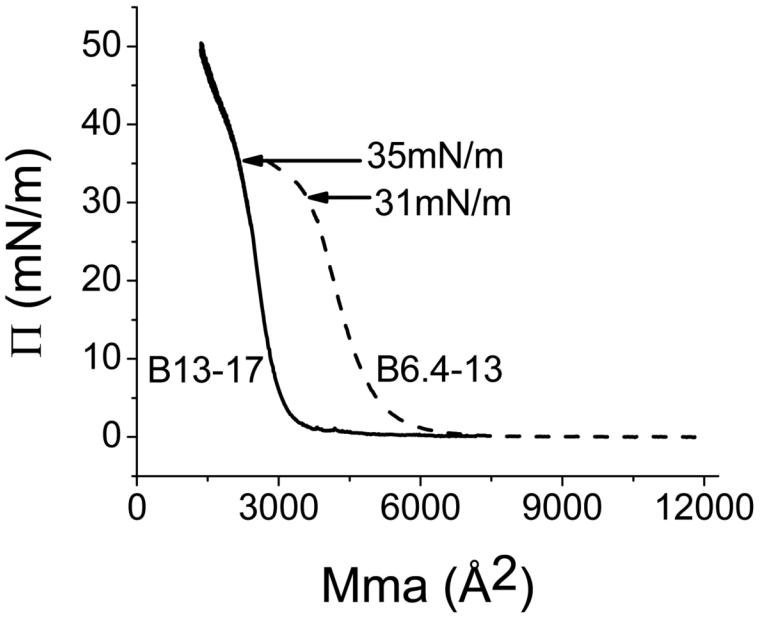

Fig. 7.

The pressure/area (Π-A) isotherm for B6.4-13 and B13-17 at an A/W interface. B6.4-13 (12 μg)or B13-17 (11.25 μg) in 30% (wt/vol) isopropanol/phosphate buffer at pH 7.4 was spread on a 3.5 M KCl/10 mM phosphate pH 7.4 sub-phase at 25°C. The monolayer was compressed at 5 mN/m per min to produce the Π-A isotherm. The lift off area is 16.6 $Å^2$/aa for B6.4-13 and 17.8 $Å^2$/aa for B13-17 ; while the collapse pressure is 31mN/m (12.2 $Å^2$/aa) for B6.4-13 and 35mN/m (13.3 $Å^2$/aa) for B13-17.

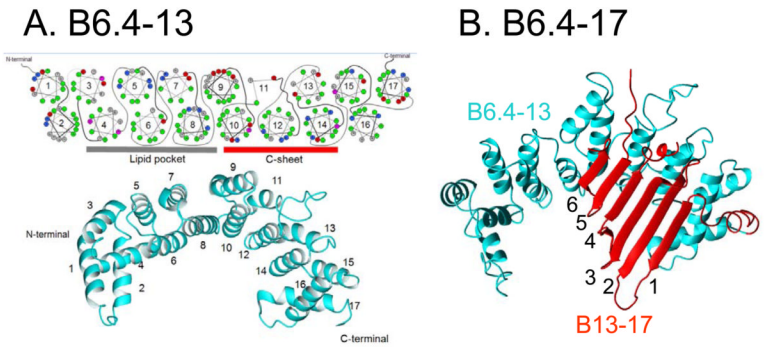

Fig. 8.

(A) B6.4–13 structural model derived from lipovitellin homology by Jiang et al (35). In this model, B6.4–13 is an α-helical domain with 17 amphipathic helices forming two layers (lower panel). The helical wheel diagram of the 17 amphipathic α-helices is shown in the upper panel. Green is hydrophobic, gray is neutral, blue is positively charged and red is negatively charged residues. There is a hydrophobic core with a hydrophobic surface created by helices 4, 6, and 8, and a positively charged surface on helices 10, 12, and 14 which stabilize the negatively charged face of the β-sheet domain B13-17 (C-sheet, red). The grey bar underneath the Edmondson wheels of helices 4, 6, and 8 marked with the "lipid pocket" indicates that helices 4-8 may form a lipid binding pocket, while the red bar underneath the Edmondson wheels of helices 10, 12 and 14 marked with "C-sheet" indicates that helices 10-14 may interact with the C-sheet. The surface area of B6.4-17 at the A/W interface is 16.6Å^2/aa indicating the 17 α-helices must all lie flat on the surface. We suggest that they also lie flat on the TO/W interface. The very hydrophobic helix 6 is most likely buried into the oil phase preventing the peptide from being pushed off the interface. (B) B6.4-17 structural model derived from lipovitellin homology by Jiang et al (35), in which B13-17 (in red) interacts with B6.4-13 (in cyan). B13-17 is a β-sheet domain consists a 6 stranded β-sheet with an un-modelled region between strands 4 and 5. The surface area of the isolated B13-17 at the A/W interface (17.8Å^2/aa) is consistent with all the amino acids interacting with the surface. We suggest that the 6 β-strands would lie flat at the TO/W interface at low and high pressure. The missing region between strand 4 and strand 5 could be the region desorbs from the interface upon compression.

Table 1

Comparison of the surface properties of B6.4-13, B13-17 and B6.4-17 (44) at TO/W and A/W interface.

	At TO/W interface							At A/W interface		
Peptides	**γ_{eq} (mN/m) at c (M)**	**Π_{MAX} (mN/m)**	**ε (mN/m) ΔV<25%**	**ϕ (degree)**	**ε′ (mN/m)**	**Exch. off**	**Pushed off**	**Limiting A ($Å^2$/aa)**	**Collapse Π (mN/m)**	**A at collapse ($Å^2$/aa)**
B6.4-13	14.1 (1.5×10^{-7})	16.7	25.6±6.5	16.5±7.7	25.6±7.1	No	Partly	16.6	31	12.2
B13-17	12.6 (1.5×10^{-7})	19.2	38.0±7.3	4.5±3.8	37.8±7.4	No	Partly	17.8	35	13.3
B6.4-17 (44)	13 (1.9×10^{-7})	16.7	32.3±3.9	10.3±4.6	31.8±4.2	No	Partly	8.6	28±1	7.3

γ_{eq}, the equilibrium interfacial tension; Π_{MAX}, the maximum pressure that peptide could withstand without being ejected from the interface; ε, visco-elastic modulus; ϕ, viscous phase angle, a phase difference between dγ and dA; ε′, elastic component, the real part of modulus; Exch. off, exchanged off, whether the peptide partly desorbs from the interface during buffer exchange procedure; Pushed off, whether the peptide desorbs from the interface when compressed the interface; Limiting A, extrapolation of the steep part of the Π-A isotherm to the baseline gives a limiting area; Collapse Π, the surface pressure at which there is a abrupt change in the slope of the Π-A isotherm above which the isotherm is not readily reversible; A at collapse, the surface area per amino acid when the peptide monolayer collapse.